JOURNAL OF MATERIALS SCIENCE 27 (1992) 5837–5843

Investigation of strontium-doped La(Cr, Mn)O_3 for solid oxide fuel cells

RASIT KOC*, H. U. ANDERSON
University of Missouri-Rolla, Ceramic Engineering Department, Rolla, MO 65401, USA

The (La, Sr) (Cr, Mn)O_3 system was investigated in an effort to develop an interconnect and cathode materials for solid oxide fuel cells. Sintering studies were done in air at temperatures below 1500 °C. Significant improvements in densification were observed with substitution of 50 mol% Mn for chromium and a density of 95% theoretical was achieved with the substitution of 70 mol% Mn for chromium in the La(Cr, Mn)O_3 system. Electrical conductivity (d.c.) measurements were made as a function of temperature and oxygen activity. At 1000 °C and 1 atm oxygen, the electrical conductivity ranged from 2.2–20 S cm^{-1} for $LaCr_{0.8}Mn_{0.4}O_3$ and $La_{0.9}Sr_{0.1}Cr_{0.2}Mn_{0.8}O_3$, respectively. All of the compositions showed similar dependence of electrical conductivity on the oxygen activity. Dependence was small at high oxygen activities; as the oxygen activity decreased, a break in electrical conductivity at 10^{-12} atm and 1000 °C was observed, and then the electrical conductivity decreased as $P_{O_2}^{1/4}$. Sintering and electrical conductivity studies indicate that $La_{0.9}Sr_{0.1}Cr_{0.3}Mn_{0.7}O_3$ appears to be a candidate for solid oxide fuel cell applications.

1. Introduction

High-temperature solid oxide fuel cells (SOFC) have been extensively investigated for a number of years, because they have the potential of converting chemical energy into electrical energy. In the US, they are being used to improve the efficiency of power generation for systems using coal or coal-derived fuels [1–6]. At the present time, the most frequently used system uses yttrium-stabilized ZrO_2 as an electrolyte, a metal or cermet as an anode, and conducting oxides as cathodes and interconnects. The features that need improvement in solid oxide fuel cells include:

1. conductivity of the electrolyte;
2. conductivity of the cathode and interconnect;
3. chemical and structural stability of the interconnect;
4. gas tightness of the interconnects;
5. thermal expansion match of cell components;
6. fabrication compatibility of the components of the cell.

The requirements for a fuel cell electrolyte are very stringent. The thermal expansion must match the other cell components. It must be chemically stable with respect to the other cell components. It must be capable of being fabricated to a nonporous density. The ions it passes must be oxygen, and the electrical conductivity must remain > 90% ionic at a level of at least 0.1 S cm^{-1} over the oxygen activity range of 10^{-18}–1 atm [3]. Although the electrical conductivity of the most successful electrolyte (yttrium-stabilized ZrO_2) could be increased, it presently represents less than 10% of the overall cell resistance; so at the moment it does not appear to limit the utilization of high-temperature fuel cells, but for improved performance, the electrical conductivity needs to be increased.

Currently, nickel-based alloys are being used for anodes; however, because of the oxidation resistance requirements, oxides are being considered. An anode represents about 25% of the resistance losses of a cell, consequently improvements in its electrical conductivity would be helpful, but the 65% contribution to resistance by the cathode, represents the primary resistance problem in the system.

A cathode has to act not only as a catalyst for the dissociation of oxygen but as an electrode as well. Applications are being found for perovskite-type oxides as cathodes because of their high electrical conductivity and catalytic activity. To be used as a cathode, a material must meet a number of requirements: it must (1) be stable towards oxidation and reduction, (2) be chemically compatible with other cell components, (3) be able to match the thermal expansion of other cell components, and (4) have electrical conductivity > 100 S cm^{-1}.

At present, $LaMnO_3$ substituted with 10–20 mol % Sr with a conductivity of about 110 S cm^{-1} at 1000 °C appears to match these requirements the best [7].

* *Present address*: National Renewable energy Laboratory, 1617 Cole Blvd., Golden, Co 80401, USA.

0022–2461

Thus, it is being used as a cathode. This material, however, contributes to high internal resistance losses in the cells (65%). A lowering of these losses would greatly enhance the effectiveness of high-temperature fuel cells. Such losses could be substantially lowered if the electrical resistance of the cathodes could be reduced by a factor of 2–5. To achieve a reduction of this magnitude requires the alteration of the conduction properties of the cathodes or changes in the material.

The stability of the cathode and interconnect to variations in the oxygen activity and temperature are of major concern. $LaMnO_3$-based cathodes and $LaCrO_3$-based interconnects are very sensitive to reduction. The oxygen loss reduces the charge carrier concentration and thereby increases the electrical resistance by about an order of magnitude.

The cathode, strontium-doped $LaMnO_3$, is less stable than $LaCrO_3$ and begins to lose oxygen and experience substantial decrease in conductivity at $P_{O_2} < 10^{-10}$ atm. In fuel gas at 1000 °C, strontium-doped $LaMnO_3$ dissociates into La_2O_3, $SrMnO_3$, and MnO and becomes structurally unsound (see Table I) [7]. Improved resistance of the cathode towards reduction was also a goal of this study.

The loss of oxygen on the fuel side of the interconnect may influence both the oxygen permeability and mechanical stability of relatively thin (1 mm thick) structures. Under reducing conditions of 10^{-20} atm, as much as 5 mol % oxygen may be lost from 10 mol % Mg-doped $LaCrO_3$. This causes about 0.1% expansion at $P_{O_2} < 10^{-16}$ atm and 1000 °C. This raises a question about the stability of the structure towards cracking as a result of the occurrence of potentially high stresses caused by the loss of oxygen. The problem is even more profound for strontium-doped $LaCrO_3$ because as much as 0.4% expansion occurs with reduction [8].

Thermal expansion mismatch between the $LaCrO_3$ and ZrO_2 appear to be the most severe problem. Table II compares the thermal expansion coefficient (TEC) of yttrium-stabilized ZrO_2 (Y–PSZ) and various $LaCrO_3$ compositions [8]. As can be seen (Table II), the TEC of magnesium-doped $LaCrO_3$ cannot be made to match Y–PSZ for any magnesium content; however, as little as 2 mol % Sr will yield a TEC match. This suggests that strontium might be a better dopant for $LaCrO_3$ than the magnesium that is currently being used [8]. The thermal expansion of the cathode, $LaMnO_3$, is higher than that of Y–PSZ (see Table III). This mismatch is a potential problem, but to date there is no evidence to support this conjecture. Perhaps the fact that the cathode is porous allows stress relief at the interface.

TABLE II Thermal expansion coefficients of interconnects (from [8])

$La_{1-x}Sr_xCrO_3$ (350–1000 °C)		$LaCr_{1-y}Mg_yO_3$ (350–1000 °C)	
Composition (x)	TEC (10^{-8} °C^{-1})	Composition (y)	TEC (10^{-8} °C^{-1})
0.02	10.24	0.00	9.48
0.05	10.89	0.02	9.46
0.10	10.74	0.05	9.57
0.15	10.84	0.10	9.48
0.20	11.10	0.15	9.55
Y-PSZ	10.30		

TABLE III Thermal expansion coefficients of cathode (from [8])

$La_{1-x}Sr_xMnO_3$ (25–1000 °C)	
Composition (x)	TEC (10^{-8} °C^{-1})
0.00	11.2
0.05	11.7
0.10	12.0
0.20	12.4
0.30	12.8

Another problem in high-temperature fuel cells is the inherent processing incompatibility of the various cell components. This problem exists for both the planar and tubular cell geometries. The Westinghouse company has tried to avoid this by using chemical vapour deposition techniques to make the cells. However, difficulties occur with the deposition of the interconnect. Evidently, porosity is a problem. The co-fired planar or tubular geometries present some real challenges, because these structures are made in a monolithic manner, e.g. for the Argonne cell, all four cell components must be sintered simultaneously and for the Westinghouse tubular cell, the cathode interconnect and support tube must be sintered simultaneously. This means for the planar cell that the dense portions, electrolyte and interconnect, must show the same sintering shrinkage as the porous anode and cathode. For the tubular cell, the interconnect must be dense, crack free and adhere to the porous substrate

TABLE I Electrical conductivity and oxygen loss of cathode and interconnect at 1000 °C as a function of oxygen activity (from [7])

P_{O_2} (atm)	$La_{0.8}Sr_{0.2}MnO_3$		$LaCr_{0.95}Mg_{0.05}O_3$	
	σ (S cm^{-1})	Oxygen lost (mol)	σ (S cm^{-1})	Oxygen lost (mol)
10^{0}	150	0	3.2	0
10^{-8}	150	0	3.2	0
10^{-10}	125	0.02	3.2	0
10^{-12}	65	0.04	3.2	0
10^{-14}	22 (dissociated)	0.15	2.5	0.004
10^{-16}	10 (dissociated)	0.20	0.32	0.017

and cathode. Moreover, all components must sinter at the same temperature and ambient atmosphere. It has been shown that $LaCrO_3$ does not densify well below 1700 °C and an oxygen activity of less than 10^{-9} atm [9]. However, the other cell components cannot withstand such severe conditions so that it is necessary to alter the sintering characteristics of the $LaCrO_3$ if the cell is to be successfully utilized. The present work addresses this problem by studying the optimization sintering of $LaCrO_3$–$LaMnO_3$ materials in air at temperatures below 1500 °C to dense ceramics without the deterioration of either the electrical conductivity or high-temperature stability through variation in the composition.

2. Experimental procedure

Specimens in the (La, Sr) (Cr, Mn)O_3 system were prepared by a polymer precursor method similar to that first described by Pechini [10]. The starting chemicals were lanthanum, strontium and manganese carbonate and chromium nitrate. All of the chemicals were reagent grade materials and were standardized by thermogravimetric methods to determine the actual cation contents. The desired compositions were prepared by dissolving measured amounts of selected carbonates and nitrates in solutions of citric acid, ethylene glycol and water. The mixtures were heated on a hot plate at about 95 °C until polymerization had occurred. Subsequent heating at higher temperatures resulted in the decomposition of the polymer resin and allowed conversion into the desired oxide. Final calcination was done at 850 °C for 8 h. The resulting powders were milled and subjected to X-ray diffraction to ensure that they were single phase. For the electrical conductivity and sintering studies the powders were pressed into bars with the aid of PVA and water binder. A compaction pressure of 2500 kg cm^{-2} yielded 0.6 cm × 0.4 cm × 3.0 cm bars with density of about 52% theoretical. Densification was conducted at 1475 °C for 11, 24, 48 h in an SiC heated furnace. Bulk densities of compositions were measured by the liquid (freon) displacement technique. Scanning electron micrographs of the polished and thermally etched surfaces of sintered specimens were taken in a model Jeolco JSM-35 CF scanning electron microscope (SEM).

Electrical conductivity and thermoelectric power measurements were made simultaneously in an apparatus which could measure three samples at a time. For these measurements the samples were cut into bars with the dimensions (0.3 cm × 0.3 cm × 2.0 cm) and electroded with platinum paste. The specimens were mounted between two platinum blocks, which had Pt–10% Rh/Pt thermocouples as electrical contacts; a platinum wire heater was wound on the lower end of the holder to generate the temperature gradient along the vertical direction. Three sets of specimens and holders were contained in Al_2O_3 tubes within an $MoSi_2$ furnace, where temperature was controlled by a Eurotherm temperature controller. The oxygen activity over the samples was controlled by using flowing gas mixtures composed of either O_2–N_2 or CO_2–forming gas ($10H_2$–$90N_2$). A stabilized zirconia oxygen sensor was used to monitor the oxygen partial pressure of the gas mixture. The Seebeck coefficient was determined by measuring temperature gradients and thermal e.m.f.s through the common leads of the thermocouples. Electrical conductivity measurements were made using the two-probe, four-wire Kelvin technique in which two leads carry the test signal (1 mA) and the other two measure the voltage drop. The measurements were made using a data logger (a Hewlett Packard 3497A data acquisition/control unit), which employs a HP-85 computer both as a control and readout device. More details on this apparatus are available in the literature [11].

3. Results and discussion

3.1. Sintering studies:

The densification of the various compositions was studied as a function of manganese content and time at 1475 °C in air. The results are illustrated in Fig. 1. It was clear that the substitution of manganese for chromium improved the sinterability of all compositions. At the present time there are no data to determine which mass transport mechanism is dominating the densification mechanism in the compositions. However, it is certain that manganese substitution for chromium in $LaCrO_3$ increased the sintered density. Significant improvement in densification was observed with substitution of 50 mol % Mn for chromium, and 95% theoretical density was achieved with substitution of 70 mol % Mn for chromium. This is probably due to the formation of Mn^{4+} ions at high manganese concentrations, which would have induced the formation of the rhombohedral structure and the creation of vacancies on the cation sites [12]. This would suggest the mass-transport activity is low when the manganese concentration is low (manganese ion probably in the 3 + stage) due to lack of ionic defects. As the manganese concentration is increased, Mn^{4+} ions will eventually form, resulting in an increase in the concentration of cation vacancies. Scanning electron micrographs of the polished and thermally etched

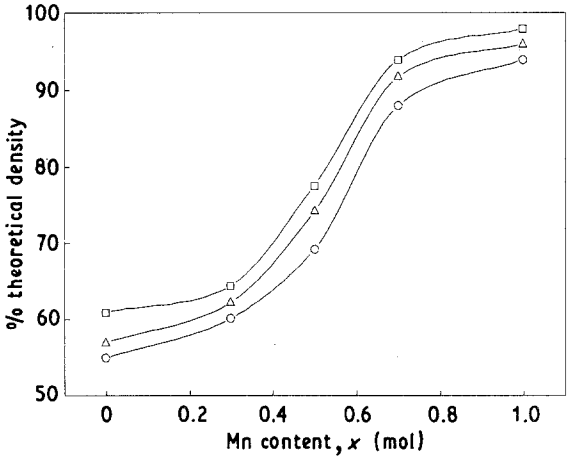

Figure 1 Sintering of compositions as a function of manganese content and time (sintering temperature 1475 °C): (□) 48 h, (△) 24 h, (○) 11 h.

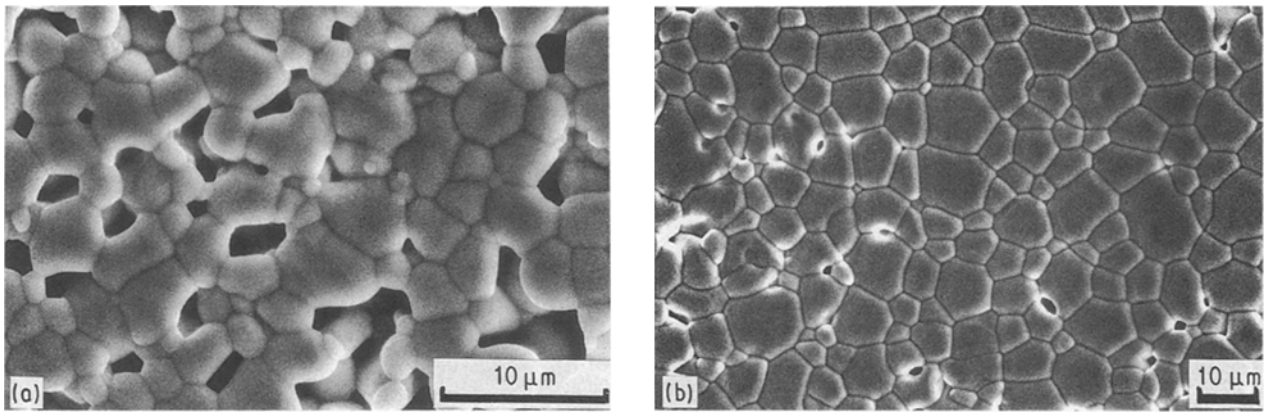

Figure 2 Scanning electron micrographs of the polished and thermally etched surfaces of $La_{0.9}Sr_{0.1}Cr_{1-x}Mn_xO_3$ sintered at 1475 °C for 48 h: (a) $x = 0.5$, (b) $x = 0.7$.

surfaces of specimens sintered at 1475 °C for 48 h are given in Fig. 2. Microstructure development with manganese substitution in $LaCrO_3$ can be observed from these photomicrographs.

3.2. Electrical conductivity and Seebeck coefficients

3.2.1. Temperature dependence

Conduction in $LaCrO_3$ and $LaMnO_3$ is thought to occur by the diffusion of p-type small polarons among chromium or manganese ions. A polaron is associated with a particular chromium or manganese site if the ion is in the + 4 valence state, rather than the stoichiometric + 3 valence state. The polaron hopping is characterized by a thermally activated mobility. When the concentration of small polarons is independent of temperature conductivity expected to take the form

$$\sigma = A/T^s \exp(-E_\alpha/kT) \quad (1)$$

where A is both a charge carrier concentration and material constant, T is the absolute temperature, $s = 1$ in the adiabatic limit and $s = 3/2$ in the non-adiabatic regime, E_α is the activation energy, and k is Boltzmann's constant. Therefore, for materials which obey the small polaron mechanism, Arrhenius plots are expected to be linear, with a slope proportional to the activation energy associated with small polaron hops. For this study, the adiabatic form was used to analyse the conductivity data.

The electrical conductivity data for $LaCr_{1-x}Mn_xO_3$ and $La_{0.90}Sr_{0.10}Cr_{1-x}Mn_xO_3$ are shown in Figs 3 and 4, respectively, as $\log\sigma$ versus reciprocal temperature. The data were similar in both systems with an order of magnitude drop in the conductivity when a small amount of manganese was substituted for chromium. Figs 5 and 6 are typical Arrhenius plots of $\log\sigma T$ versus reciprocal temperature. The activation energies for motion of charge carriers determined from Figs 5 and 6 are plotted in Fig. 7 as a function of manganese content. The end members of the series, $LaCrO_3$ and $LaMnO_3$, exhibit small polaron behaviour over a wide temperature range and have very similar activation energies. The

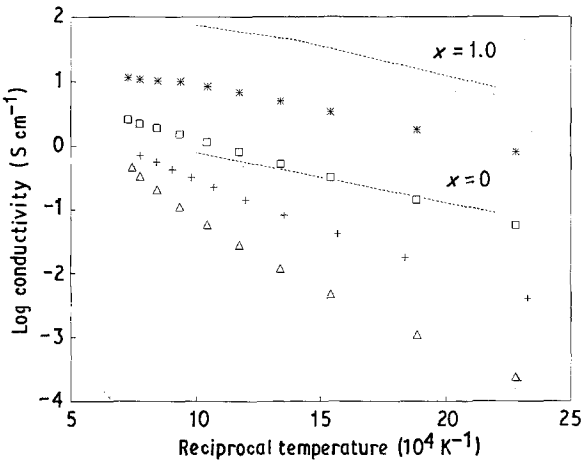

Figure 3 Electrical conductivity of $LaCr_{1-x}Mn_xO_3$ as a function of temperature. (– – –) End members. x: (△) 0.2, (+) 0.3, (□) 0.4, (*) 0.6.

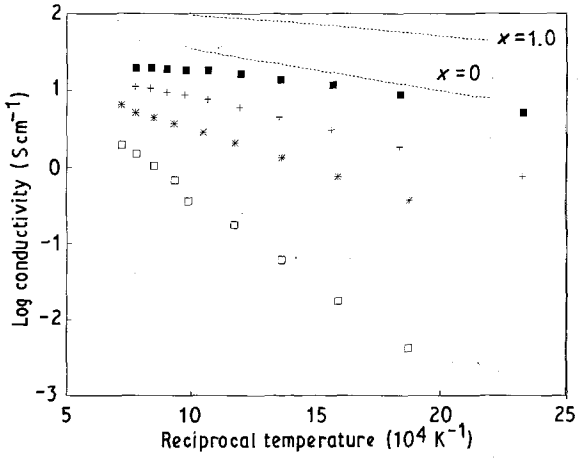

Figure 4 Electrical conductivity of $La_{0.9}Sr_{0.1}Cr_{1-x}Mn_xO_3$ as a function of temperature. (– – –) End members. x: (□) 0.2, (*) 0.4, (+) 0.6, (■) 0.8.

conductivity of undoped $LaMnO_3$ is about 400 times greater than that of $LaCrO_3$. A least squares fit to the data gives an activation energy of 0.18 eV for $LaCrO_3$ and 0.19 eV for $LaMnO_3$. The linearity of the data for

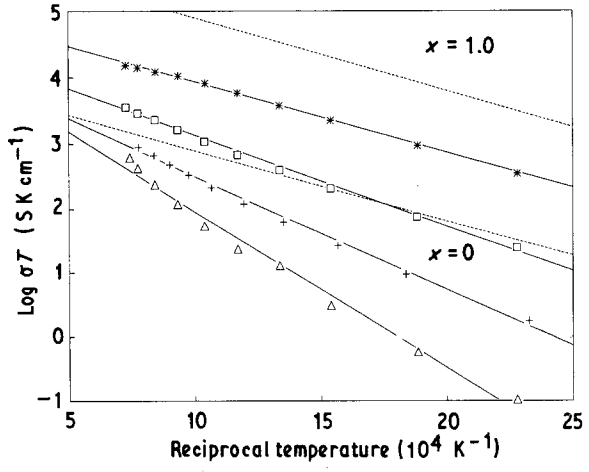

Figure 5 Log σT versus reciprocal temperature for $LaCr_{1-x}Mn_xO_3$. (– – –) End members, (———) theoretical fits to the data. x: (△) 0.2, (+) 0.3, (□) 0.4, (*) 0.6.

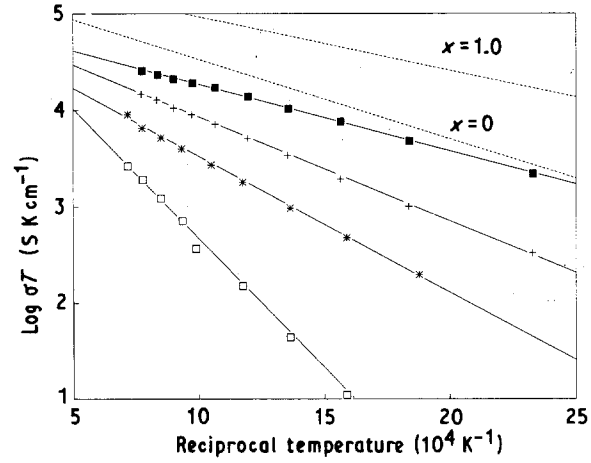

Figure 6 Log σT versus reciprocal temperature for $La_{0.9}Sr_{0.1}Cr_{1-x}Mn_xO_3$. (– – –) End members, (———) theoretical fits to the data. x: (□) 0.2, (*) 0.4, (+) 0.6, (■) 0.8.

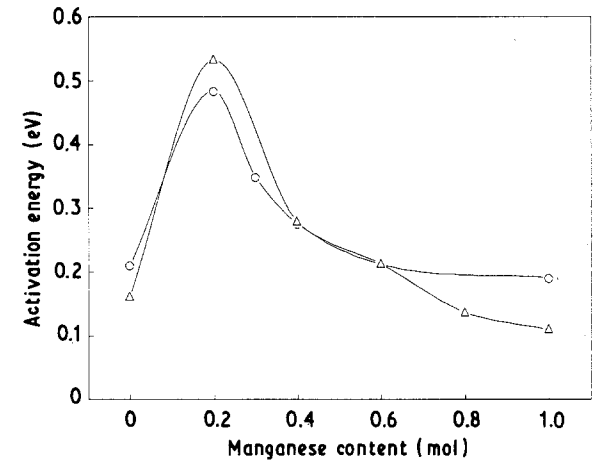

Figure 7 Activation energy for conduction versus manganese content in (La, Sr)$Cr_{1-x}Mn_xO_3$. (△) 10% Sr, (○) 0% Sr.

the end members over such an extended temperature range is consistent with the earlier identification of the conductivity in these materials as being due to a temperature-independent concentration of p-type small polarons. In spite of the larger intrinsic electronic conductivity of $LaMnO_3$, a small substitution of manganese for chromium in $LaCrO_3$ results in a sharp drop in low-temperature conductivity from that exhibited by either end member. This minimum, which at room temperature is more than four orders of magnitude below that of $LaCrO_3$, occurs at a manganese concentration of 20 mol %. In addition, these small substitutions of manganese result in a nonlinear temperature dependence with increased slope. The maximum slope observed occurs in the 20 mol % Mn composition and corresponds to an activation energy of 0.48 eV. As can be seen from Fig. 7, the activation energy increases with manganese content to maximum at 20 mol % and then linearly decreases as the manganese content increases. The substitution of small amounts of manganese for chromium have been found to cause the room-temperature electrical conductivity to drop orders of magnitude below that of either end member and increase in activation energy. This behaviour is attributed to a lower small polaron site energy at the manganese sites as compared to chromium sites. At low manganese concentrations, the lower energy manganese sites act as traps for carriers diffusing among chromium sites. Therefore, the activation energy for conduction is increased from that of $LaCrO_3$. At higher manganese concentrations, direct transport among manganese sites becomes possible and the conductivity increased and activation energy decreased.

Thermopower measurements were made to determine the type and concentration of charge carriers. Figs 8 and 9 show plots of the Seebeck coefficients versus temperature for $LaCr_{1-x}Mn_xO_3$ and $La_{0.9}Sr_{0.1}Cr_{1-x}Mn_xO_3$, respectively. The Seebeck measurements exhibit similar behaviour with respect to manganese substitution for chromium in both the undoped and strontium-doped series. There is an appropriate shift in the magnitude of the Seebeck coefficient with strontium addition in $LaCrO_3$; however, very little occurs in the manganese substituted compositions. The Seebeck coefficients show essentially no change with the 10 mol % Sr substitution for the compositions containing more than 30 mol % Mn.

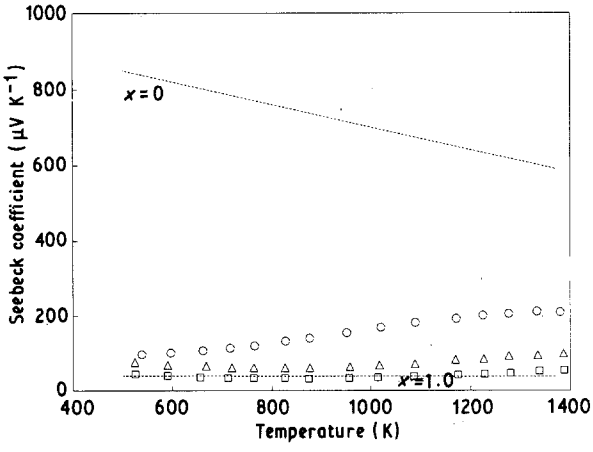

Figure 8 Seebeck coefficient versus temperature for $LaCr_{1-x}Mn_xO_3$. (– – –) End members. x: (○) 0.2, (△) 0.4, (□) 0.6.

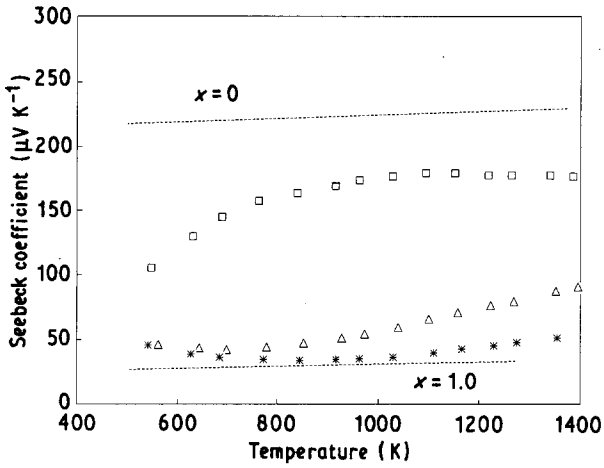

Figure 9 Seebeck coefficient versus temperature for $La_{0.9}Sr_{0.1}Cr_{1-x}Mn_xO_3$ (– – –) End members. x: (□) 0.2, (△) 0.4, (*) 0.6.

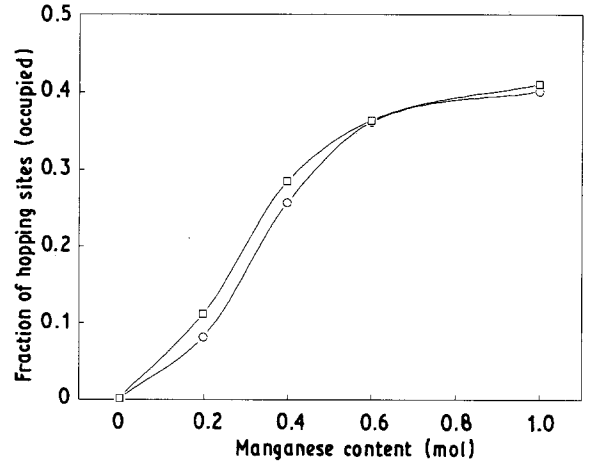

Figure 10 Calculated fraction of occupied hopping sites as a function of manganese content at 1000 °C for $LaCr_{1-x}Mn_xO_3$. (○) 0% Sr, (□) 10% Sr.

This indicates that strontium substitution to compositions containing more than 30 mol % Mn probably did not result in the formation of conducting small polarons at the chromium or manganese sites in accordance with Verway *et al.*'s principle [13]. Therefore, the absence of significant increase in the electrical conductivity and decrease in the high-temperature Seebeck coefficients were observed for compositions containing more than 30 mol % Mn. Seebeck coefficients have a non-linear temperature dependence for the mixed compositions. The Seebeck coefficients of end members are linear with respect to temperature. According to Heikes's formula this type of behaviour indicates a small polaron conduction mechanism. (Heikes's formula is a temperature-independent expression.) Using the assumption that only one electron is allowed on a given site and both spin and orbital degeneracy are negligible, yields an expression for the Seebeck coefficient [14]

$$Q = (k/e)\{\ln[(1 - x)/x] + S^*/k\} \qquad (2)$$

where k is Boltzmann's constant, e is the unit charge, x is the fraction of hopping sites which are occupied and S^* is the vibrational entropy associated with the ions surrounding a polaron on a given site. This equation leads to a temperature-independent Seebeck coefficient. Usually, the entropy, S^*, is small enough to be negligible; therefore, the Seebeck coefficient depends only on the concentration term. Using the Seebeck data and Heikes's formula, the fraction of hopping sites at 1000 °C was calculated as a function of manganese substitution (Fig. 10). As can be seen, the fraction of occupied hopping sites increased as a function of manganese substitution. This behaviour agreed with the electrical conductivity.

3.2. Oxygen activity dependence

D.c. electrical conductivity measurements for $LaCr_{0.4}Mn_{0.6}O_3$, $La_{0.9}Sr_{0.1}Cr_{0.4}Mn_{0.6}O_3$, and $La_{0.9}Sr_{0.1}Cr_{0.6}Mn_{0.4}O_3$, were made as a function of oxygen activity at 1000 °C. The results are shown in Fig. 11 in which $La_{0.9}Sr_{0.1}MnO_3$ and $LaCr_{0.95}Mg_{0.05}O_3$ data are included for comparison. The electrical conductivity data showed similar oxidation–reduction behaviour. In the high oxygen activity region, within experimental error, the electrical conductivity was nearly constant. The conductivity decreased as a function of oxygen activity to the one-quarter power as reduction progressed. The constant electrical conductivity which exists in the high oxygen activity region may be easily understood if it is assumed that the carrier concentration and electronic compensation predominates. In the low oxygen activity region, oxygen vacancies are formed and the electrical conductivity begins to decrease as a result of ionic compensation.

Seebeck measurements were also made as a function of oxygen activity at 1000 °C for some compositions. It was found that the Seebeck coefficients were always positive even after the compounds decomposed. At 1000 °C with decreasing oxygen activity, the Seebeck coefficients increased to a maximum then started decreasing as a result of decomposition. The critical oxygen activity for compositions were observed to be close to those for $LaMnO_3$ (about

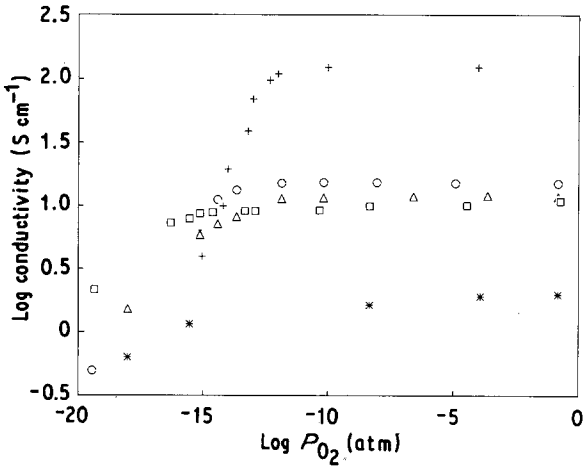

Figure 11 Log conductivity versus log P_{O_2} for compositions at 1000 °C. (+) 10% Sr–$LaMnO_3$, (*) 5% Mg–$LaCrO_3$, (○) 10% Sr, 60% Mn, (△) 10% Sr, 40% Mn, (□) 0% Sr, 60% Mn.

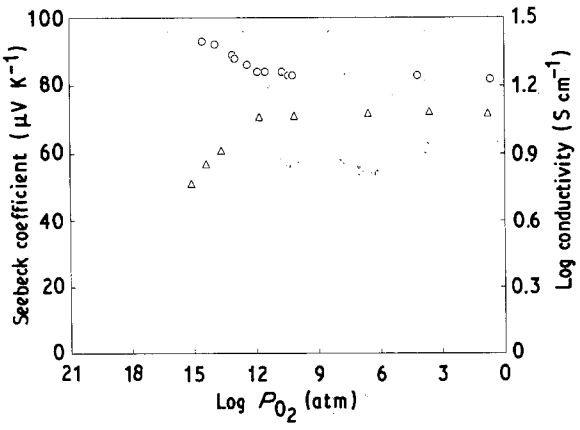

Figure 12 (○) Seebeck coefficient and (△) log conductivity as a function of oxygen activity at 1000 °C for $La_{0.9}Sr_{0.1}Cr_{0.6}Mn_{0.4}O_3$.

10^{-15} atm at 1000 °C). An initial drop in the electrical conductivity of compositions was observed as oxygen activity was decreased. This must be due to the reduction in the number of charge carriers as oxygen vacancies were introduced. This was confirmed by the oxygen activity dependence of the Seebeck coefficient at 1000 °C. Fig. 12 shows the experimental evidence of such a relationship between conductivity and Seebeck coefficient for $La_{0.9}Sr_{0.1}Cr_{0.6}Mn_{0.4}O_3$. As can be seen in Fig. 12, the Seebeck coefficient increased and the electrical conductivity decreased with decreasing oxygen activity. This was true until decomposition occurred.

4. Conclusion

The $LaCrO_3$–$LaMnO_3$ system forms a solid solution. Manganese substitution for chromium in $LaCrO_3$ significantly improved the sinterability in air. Densities above 95% theoretical were achieved at 1475 °C for composition $La_{0.9}Sr_{0.1}Cr_{0.3}Mn_{0.7}O_3$. However, the substitution of such quantities of manganese on the chromium site has shown two negative effects:

1. electrical conductivity decreased;
2. stability against reduction was obtained only at very high chromium concentrations ($La_{0.9}Sr_{0.1}Cr_{0.8}Mn_{0.2}O_3$).

References

1. T. TAKHASHI, in "Physics of Electrolytes", edited by J. Haadik (Academic Press, New York, 1972) p. 989.
2. A. O. ISENBERG, *Solid State Ionics* **3/4** (1981) 432.
3. I. J. ROHR, in "High Temperature Fuel Cells", edited by P. Hagenmuller and W. Van Gool (Academic Press, New York, 1987) p. 431.
4. W. FEDUSKA and A. O. ISENBERG, *J. Power Sources* **10** (1983) 89.
5. M. WARSHAY, "Discussion of Potential of High Temperature Solid Oxide Fuel Cell Power Plan Systems", in the Workshop on High Temperature Solid Oxide Fuel Cells, Brookhaven National Laboratory, Upton, New York, 5–6 May 1977.
6. D. C. FEE, "Solid Oxide Fuel Performance", in Proceedings of the Conference on High Temperature Solid Oxide Electrolytes, Brookhaven National Laboratory, Upton, New York, 16–18 August 1983, edited by D. Fee, J. Fillo and H. Isaacs, p. 4.
7. L. KUO, PhD thesis, University of Missouri-Rolla (1987).
8. S. SRILOMSAK, D. P. SCHILLING, H. U. ANDERSON, in "Proceedings of the 1st International Conference on Solid Oxide Fuel Cells", Hollywood, Florida, October 1989, edited by S. C. Singhal (The Electrochemical Society, NJ, 1989) p. 129.
9. L. GROUPP and H. U. ANDERSON, *J. Amer. Ceram. Soc.* **59** (1976) 449.
10. M. PECHINI, US Pat. 3 330 697 (1967).
11. G. CARINI, MS thesis, University of Missouri-Rolla (1988).
12. R. KOC, H. U. ANDERSON, S. A. HOWARD and D. M. SPARLIN, in "Proceedings of the 1st International Conference on Solid Oxide Fuel Cells", Hollywood, Florida, October 1989, edited by S. C. Singhal (Electrochemical Society, NJ, 1989) p. 220.
13. E. J. VERWAY, P. W. HAAIJAM, F. C. ROMEIJH and G. W. VAN OOSTERHOUT, *Philips Res. Report* **5** (1950) 173.
14. R. R. HEIKES, in "Thermoelectricity: Science and Engineering" edited by R. R. Heikes and R. W. Ure, Jr (Wiley Interscience, New York, 1961) p. 37.

Received 14 August
and accepted 28 November 1991